Boundary layer flow and heat transfer of a modified second grade nanofluid with new mass flux condition

Masood ur Rahman [a,b,*], Masood Khan [b], Mehwish Manzur [b]

[a] Department of Applied Mathematics, Western University, Middlesex College, 1151 Richmond Street, London, Ontario, Canada
[b] Department of Mathematics, Quaid-i-Azam University, Islamabad 44000, Pakistan

ARTICLE INFO

ABSTRACT

The purpose of the current problem is to analyze the nano boundary layer flow and heat transfer of the modified second grade fluid over a non-linearly stretching surface. A newly introduced boundary condition of zero nanoparticle mass flux is incorporated for the analysis. The appropriate local similarity transformations are employed to transform the modeled partial differential equations of momentum, temperature and concentration into coupled non-linear ordinary differential equations. The governing boundary value problem is numerically integrated by the help of shooting method along with Runge-Kutta Fehlberg scheme. The ascendancy of arising thermophysical parameters on the temperature and concentration profiles is graphically displayed. The detail study reveals that a decay in the nanoparticle concentration profile is found for growing values of the Brownian motion parameter while the increasing values of the thermophoresis parameter results in increment of the concentration of nanofluid. Moreover, the nanoparticle concentration became weaker with the developing values of the Lewis number. In addition, the numerical results are validated by providing exact solutions for special case and excellent compatibility between the two results is achieved.

Introduction

In the last two decades, the notion of nanotechnology has been universally exploited in the problems ascribing the conventional heat transfer in order to boost the heat transfer characteristics of several fluids. Nanofluids are basically very stable colloidal suspensions composed of nanometer sized particles termed as nanoparticles (1−100 nm) which have considerably large surface area due to which they are probable for enhancing the heat transfer rate. On account of a remarkable increase in thermal conductivity, nanofluids found practical utility in industrial, technological and various pharmaceutical processes. Nanofluids are primarily used as coolants in transformers, vehicles, computers and many other electronic devices. Nanotechnology is efficiently applied in designing various military devices, nuclear reactors, space technology and also utilized in treating several diseases like cancer infected tissues. Choi [1] bestowed a theoretical model for the enrichment of thermal transport properties of nanofluids with base fluid. He succinctly described the technology for the production of nanoparticles and reconnoiter the fact that these fluids have hefty perti-

nence for many industries. Buongiorno [2] scrutinized various mechanisms that could be authoritative for the noteworthy increase in convective heat transfer in nanofluids. Out of those slip mechanisms, thermophoresis and Brownian diffusion are much significant in nanofluids. Buongiorno presented a model for convective transport in nanofluid in order to cope with the problems which were originating in previous dispersion models. Kim et al. [3] summarized that a paramount increase in critical heat flux (CHF) can be attained at a small-scale nanoparticles concentration that is even less than 0.1% by volume. Kuznetsov and Nield [4] constructed a similar solution for the natural convection boundary layer flow of nanofluid over a vertical plate using the Buongiorno's model. Khan and Pop [5] critiqued the numerical solution for the laminar flow of a nanofluid over a linearly stretching surface. A similarity solution was constructed embodying the consequence of Brownian motion and thermophoresis. The analytical as well as numerical solutions for the flow of a nanofluids over stretching surfaces were established by Gorder et al. [6]. Roberts and Walker [7] framed out the convective performance of nanofluids in commercially procurable liquid systems for computational processing units (CPUs). The obtained results showed the same desired outcome in real systems as they take on for experimental systems. Makinde and Aziz [8] devoted their study to seek the numerical solutions for the boundary layer flow of nanofluid induced due to

---

* Corresponding author at: Department of Applied Mathematics, Western University, Middlesex College, 1151 Richmond Street, London, Ontario, Canada.
E-mail address: murrahm2@uwo.ca (M.ur Rahman).

a stretching sheet by taking into account the convective heating boundary condition. An extensive study of convective transport in nanofluid over a convectively heated surface was set up by Aziz and Khan [9]. Das et al. [10] performed a numerical investigation to probe the influence of thermal radiation on the flow of a nanofluid over an unsteady heated stretching surface. Aly and Vajravelu [11] surveyed the consequence of the second order slip condition on the nano boundary layer flows through a porous medium over stretching surfaces and thus calculated the exact and numerical solutions in the presence of transverse magnetic field. Mabood and Mastroberardino [12] contemplated the development of MHD boundary layer flow and melting heat transfer of water based nanofluid. The consequence of viscous dissipation on the electrically conducting fluid over a stretching sheet is demonstrated and the numerical solutions are constructed by Runge-Kutta Fehlberg method. Haq et al. [13] summarized the impact of combine effects of velocity and thermal slip on the MHD boundary layer flow of nanofluid considering the effect of zero normal flux of nano particles at the wall. Numerical investigations are performed by incorporating the development of stagnation point flow by taking the thermal radiation effect into account.

Due to diversified applicability of non-linear fluid flows in industrial and technological fields, researchers have advised distinct non-Newtonian fluid models [14–25] based on different constitutive relations. Amongst these models the power-law model is broadly used to envision the shear-thinning and thickening characteristics. Likewise, second grade fluid being an elementary subclass of differential type fluid can competently visualize the normal stress effects. Subsequently, a renowned model is proposed by Man and Sun [26] known as generalized second grade fluid, by combining both the second grade model and the power-law model. Generalized second grade model not only anticipates the shear-thinning and shear-thickening regimes but can also execute the normal stress behavior of fluids since the viscosity could be a function of rate of deformation. Aksoy et al. [27] computed the boundary layer equations for the modified second grade fluid and integrated them using a numerical finite difference technique to obtain the stretching sheet solutions. This work was further extended by Khan and Rahman [28] in consideration of boundary layer flow and heat transfer of modified second grade fluid over a non-linear stretching sheet. Some latest work on the modified second grade fluid includes [29–31].

The present work is based on the boundary layer flow and heat transfer of modified second grade nanofluid. The stretching solutions are computed numerically using a more realistic condition [32,33] when the nanofluid particle concentration is not intensely controlled on the boundary even though it is passively allowed. The mathematical model is developed and solved numerically by the shooting method along with Runge-Kutta Fehlberg scheme. The important results are tabulated and graphically portrayed.

Mathematical model

Governing equations

A steady two-dimensional boundary layer flow and heat transfer of a modified second grade nanofluid is designed over a non-linear stretching surface coinciding with the plane $y = 0$ while the flow would be perpendicular to the plane of the sheet (i.e. $y \geqslant 0$). The sheet being put up at a constant temperature T_w is continuously stretched with a non-linear velocity $u = cx^s$ where c, $s > 0$ such that s represents the stretching rate of the sheet and c symbolize the power-law exponent parameter. The mass flux of the nanoparticles at the wall is taken to be zero while for consid-

erably large value of y, the ambient values of concentration and temperature are C_∞ and T_∞, respectively.

The extra stress tensor τ for the modified second grade fluid satisfies [15]

$$\tau = -p\mathbf{I} + \mu\Pi^{\frac{m}{2}}\mathbf{A}_1 + \alpha_1\mathbf{A}_2 + \alpha_2\mathbf{A}_1^2, \tag{1}$$

where p is the pressure, m, α_1, α_2 and μ are the material constants, while $\Pi = \left|\frac{1}{2}tr\mathbf{A}_1^2\right|$ with $\mathbf{A}_1$ and $\mathbf{A}_2$ being the first and second Rivlin-Ericksen tensors, respectively.

For the problem under consideration, the governing conservation equations of mass, momentum, energy and concentration for the flow of an incompressible modified second grade nanofluid [27,28] take the form

$$\frac{\partial u}{\partial x} + \frac{\partial v}{\partial y} = 0, \tag{2}$$

$$\rho\left(u\frac{\partial u}{\partial x} + v\frac{\partial u}{\partial y}\right) = -\frac{\partial p}{\partial x} + \mu\left[\frac{\partial^2 u}{\partial y^2}\left|\frac{\partial u}{\partial y}\right|^m + \frac{\partial u}{\partial y}\frac{\partial}{\partial y}\left(\left|\frac{\partial u}{\partial y}\right|^m\right)\right]$$
$$+ \alpha_1\left[v\frac{\partial^3 u}{\partial y^3} + u\frac{\partial^3 u}{\partial x\partial y^2} + \frac{\partial u}{\partial x}\frac{\partial^2 u}{\partial y^2} - \frac{\partial u}{\partial y}\frac{\partial^2 u}{\partial x\partial y}\right], \tag{3}$$

$$u\frac{\partial T}{\partial x} + v\frac{\partial T}{\partial y} = \frac{k_f}{(\rho c)_f}\frac{\partial^2 T}{\partial y^2} + \tau\left[D_B\frac{\partial C}{\partial y}\frac{\partial T}{\partial y} + \frac{D_T}{T_\infty}\left(\frac{\partial T}{\partial y}\right)^2\right], \tag{4}$$

$$u\frac{\partial C}{\partial x} + v\frac{\partial C}{\partial y} = D_B\frac{\partial^2 C}{\partial y^2} + \frac{D_T}{T_\infty}\frac{\partial^2 T}{\partial y^2}. \tag{5}$$

In the above equations u and v, respectively, display the components of velocity in the x- and y-directions, T and C characterize the temperature and the nanoparticle volume fraction, m the power-law index, α_1 the material moduli, k_f the thermal conductivity and c_f the specific heat of the fluid at constant pressure. Moreover, D_B corresponds to the Brownian diffusion coefficient, D_T the thermophoresis diffusion coefficient and $\tau\left(=\frac{(\rho c)_p}{(\rho c)_f}\right)$ the ratio of effective heat capacity of the nanoparticle material (i.e $(\rho c)_p$) to heat capacity of the fluid (i.e $(\rho c)_f$).

Boundary conditions

The relevant velocity, temperature and concentration boundary conditions associated with the physical problem under discussion are

$$u(x,y) = U = cx^s, \quad v(x,y) = 0, \quad T(x,y) = T_w, \quad C(x,y)$$
$$= D_B\frac{\partial C}{\partial y} + \frac{D_T}{T_\infty}\frac{\partial T}{\partial y} \text{ at } y = 0, \tag{6}$$

$$u(x,y) \to 0, \quad \frac{\partial u(x,y)}{\partial y} \to 0, \quad T(x,y) \to T_\infty, \quad C(x,y) \to C_\infty \text{ as } y \to \infty. \tag{7}$$

It is worth noting that for $\alpha_1 = 0$, Eqs. (2)–(7) reduce to the boundary layer equations for power-law nanofluid over non-linear stretching sheet. Furthermore, for $m = 0$ they correspond to the second grade nanofluid problem and for $m = \alpha_1 = 0$, we get the nano-boundary layer equations for Newtonian fluid.

Non-dimensionalization

The governing partial differential equations can be reduced to corresponding ordinary differential equations by incorporating the following local similarity transformations

$$\eta = \frac{y}{x}\,\mathrm{Re}^{\frac{1}{2+m}}, \quad \psi = xUR e^{-\frac{1}{2+m}}f(\eta), \quad \theta(\eta) = \frac{T - T_\infty}{T_w - T_\infty}, \quad \phi(\eta)$$
$$= \frac{C - C_\infty}{C_\infty}, \tag{8}$$

where ψ is the stream function defined in the usual way as $u = \frac{\partial \psi}{\partial y}$ and $v = -\frac{\partial \psi}{\partial x}$ and Re denotes the local Reynolds number given by

$$\mathrm{Re} = \frac{\rho x^{1+m} U^{1-m}}{\mu}. \tag{9}$$

Substitution of Eq. (8) identically satisfies the continuity equation while Eqs. (3)–(5) reduces to the following system of non-linear differential equations

$$(1 + s + 2ms)ff'' + (m + 2)[(m + 1)f'''(-f'')^m - s(f')^2] \tag{10}$$

$$-k[(3s - 1)((f'')^2 - 2f'f''') + (1 + s + 2ms)ff^{iv}] = 0, \tag{11}$$

$$\theta'' + \Pr\left(\frac{1 + s + 2ms}{m + 2}\right)f\theta' + \Pr N_b\phi'\theta' + \Pr N_t\theta'^2 = 0, \tag{12}$$

$$\phi'' + PrLe\left(\frac{1 + s + 2ms}{m + 2}\right)f\phi' + \frac{N_t}{N_b}\theta'' = 0. \tag{13}$$

The transformed boundary conditions take the form

$$f(\eta) = 0, \quad f'(\eta) = 1, \quad \theta(\eta) = 1, \quad N_b\phi'(\eta) + N_t\theta'(\eta) = 0 \quad \text{at } \eta = 0, \tag{14}$$

$$f'(\eta) \to 0, \quad \theta(\eta) \to 0, \quad \phi(\eta) \to 0 \quad \text{as } \eta \to \infty, \tag{15}$$

where prime symbolizes the differentiation with respect to the local similarity variable η. The parameters k, $\Pr$, Le, N_b, N_t defines the generalized second grade parameter, the generalized Prandtl number, the Lewis number, the Brownian motion parameter, the thermophoresis parameter, respectively, given by

$$k = \frac{\alpha_1\,\mathrm{Re}^{\frac{2}{2+m}}}{\rho x^2}, \quad \Pr = \frac{Ux}{\left(\frac{k_1}{\rho c_p}\right)}\,\mathrm{Re}^{-\frac{2}{2+m}}, \quad Le = \frac{\nu}{D_B},$$
$$N_b = \frac{\tau D_B C_\infty}{\nu}, \quad N_t = \frac{\tau D_T (T_w - T_\infty)}{T_\infty \nu}. \tag{16}$$

Physical quantities of pre-eminent interest

The physical quantities of notable importance are the local skin friction coefficient C_{f_x}, the local Nusselt number Nu_x given by

$$C_{f_x} = \frac{\tau_w}{\frac{1}{2}\rho U^2}, \quad Nu_x = \frac{xq_w}{k_f(T_w - T_\infty)}, \tag{17}$$

where τ_w is the wall shear stress, q_w the wall heat flux and j_w the wall shear stress, formulated as

$$\tau_w = \left[\mu\left|\frac{\partial u}{\partial y}\right|^m \frac{\partial u}{\partial y} + \alpha_1\left(u\frac{\partial^2 u}{\partial x \partial y} + v\frac{\partial^2 u}{\partial y^2} + 2\frac{\partial u}{\partial x}\frac{\partial u}{\partial y}\right)\right]_{y=0},$$
$$q_w = -k_f\left(\frac{\partial T}{\partial y}\right)\bigg|_{y=0}. \tag{18}$$

The non-dimensional representation of the above quantities can be written as

$$-\frac{1}{2}\,\mathrm{Re}^{\frac{1}{m+2}}C_{f_x} = \frac{(1 - (7 + 2m)s)k}{m + 2}f''(0) + [-f''(0)]^{m+1},$$
$$-\mathrm{Re}^{-\frac{1}{m+2}}Nu_x = \theta'(0). \tag{19}$$

The reduced Sherwood number which represents the dimensionless mass flux at the wall is identically zero for the problem under consideration.

Solution methodology

The numerical solution

The governing equations for flow and heat transfer of modified second grade nanofluid is numerically handled by the help of Runge-Kutta Fehlberg method. The governing problem is reduced to corresponding initial value problem and the values of the missing initial conditions are calculated by Newton's method.

$$\begin{pmatrix} f_1' \\ f_2' \\ f_3' \\ f_4' \\ \\ f_5' \\ f_6' \end{pmatrix} = \begin{pmatrix} f_2 \\ f_3 \\ f_4 \\ [(1 + s + 2ms)*f_1*f_3 + (m + 2)\{(m + 1)(-f_3)^m f_4 - s(f_2)^2\} \\ -k\{(3s - 1)((f_3)^2 - 2*f_2*f_4)\}]) \\ [(1 + s + 2ms)f_1] \\ y_5 \\ -\Pr\left(\frac{1+s+2ms}{m+2}\right)f_1*f_6 - \Pr*N_b*f_6*f_8 - \Pr*N_t*f_6^2 \\ -\Pr*Le\left(\frac{1+s+2ms}{m+2}\right)f_1*f_8 - \frac{N_t}{N_b}y_6' \end{pmatrix}, \tag{20}$$

with initial conditions

$$\begin{pmatrix} f_1 \\ f_2 \\ f_3 \\ f_4 \\ f_5 \\ f_6 \\ f_7 \\ f_8 \end{pmatrix} = \begin{pmatrix} 0 \\ 1 \\ s_1 \\ s_2 \\ 1 \\ s_3 \\ -\frac{N_t}{N_b}s_3 \\ s_4 \end{pmatrix}. \tag{21}$$

Verification of numerical solutions

The appropriateness of numerical scheme is verified in Table 1 by computing the exact solutions and thus providing the comparison between the numerical solutions and exact solutions for special case. The numerical values of $-f''(0)$ and $-\theta'(0)$ are tabulated for the case of second grade fluid ($m = 0$) and for linear stretching ($s = 1$) in the absence of nanoparticles. Both the solutions are found to be in good agreement and thus our numerical methodology is verified.

Results and discussion

This section marks the physical interpretation of the behavior of the physical parameters which arise in the flow and heat transfer of the modified second grade nanofluid past a stretching surface. The numerical computation namely the shooting method along with Runge-Kutta Fehlberg scheme is incorporated to integrate the governing mathematical model. In the calculations, the default values of different parameters are taken to be $s = 1$, $k = 0.5$, $N_b = 0.5$, $N_t = 0.5$, $\Pr = 10$ and $Le = 10$ unless otherwise specified.

Fig. 1 analyses the impact of the power-law index m on the temperature and nanoparticle volume fraction distributions for the case of linear and quadratic stretching. An inspection of the graphical behavior illustrates that an increment in the value of the power-law index descends the thermal as well as concentration boundary layers. It is further revealed that the thermal as well as concentration boundary layer thickness is greater for the case of linear stretching.

Fig. 2 highlights the effect of the thermophoresis parameter N_t on the temperature and concentration fields for different values

Table 1
Comparison of the variation of $-f''(0)$ and $-\theta'(0)$ for the case of the second grade fluid ($m = 0$) when $s = 1$.

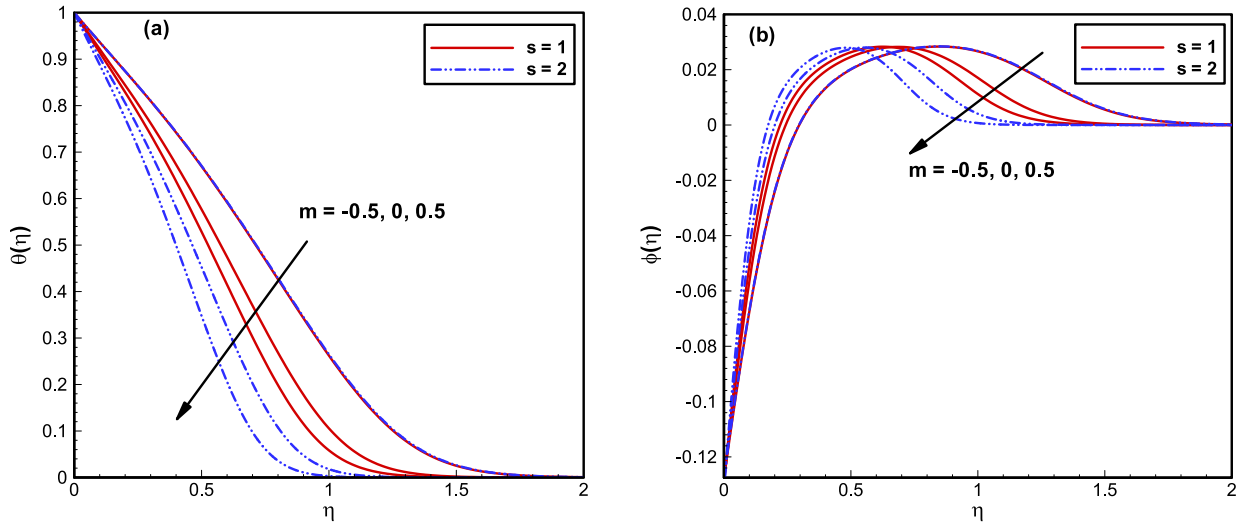| k	Pr	Exact solution		Numerical Solution	
		$-f''(0)$	$-\theta'(0)$	$-f''(0)$	$-\theta'(0)$
0.5	10	0.81649658	2.3478745	0.81651160	2.3478704
1		0.70710678	2.3715683	0.70716177	2.3715544
1.5		0.63245553	2.3877034	0.63257670	2.3876736
2		0.57735027	2.399595	0.57755736	2.3995450
	2		0.95141934		0.9514135
	5		1.6081636		1.6081591
	7		1.9354025		1.9353982

Fig. 1. Impact of the power-law index m on the temperature and concentration profiles.
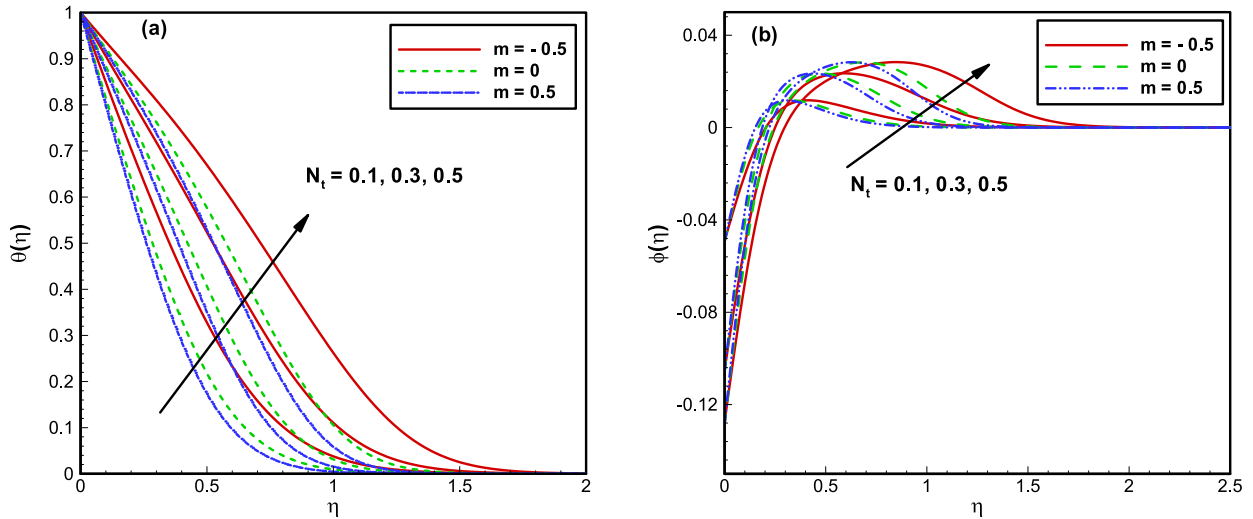

Fig. 2. Impact of the thermophoresis parameter N_t on the temperature and concentration profiles.

of the power-law index. The temperature together with the concentration of the nanofluid is increasing function of N_t. The escalated values of N_t lead to enrichment of thermophoresis force which causes the diffusion of nanoparticles in the ambient fluid due to temperature gradient resulting in the thickening of thermal and concentration boundary layers. It is noticeable that a boost in the thermophoretic effect points deeper penetration of nanoparticles in the ambient fluid causing an increase in nanofluid's temperature and concentration. Further, the thermal as well as

concentration boundary layer structures are dominant for shear-thinning fluids.

Fig. 3(a) describe the development of the temperature distribution corresponding to their dependence on the generalized Prandtl number Pr. It is visualized from these plots that an uprise in the values of Pr tends to diminish the thermal boundary layer. From the physical point of view, the thermal diffusivity becomes weaker on increasing the values of Pr which restrain the flow of heat into the fluid resulting in thinning of thermal boundary layer. Fig. 3(b)
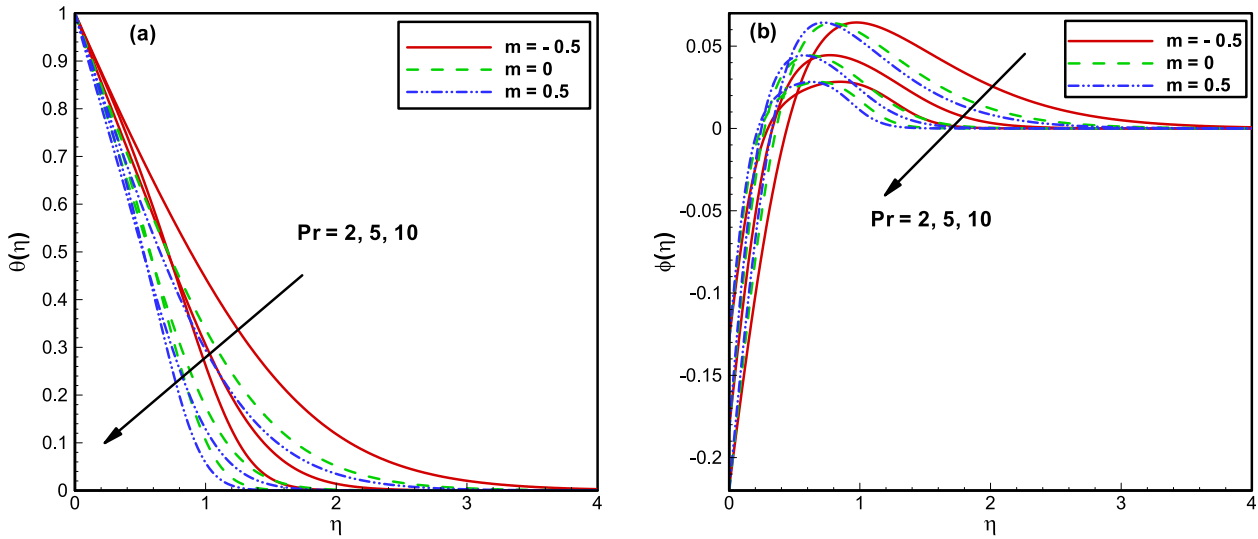
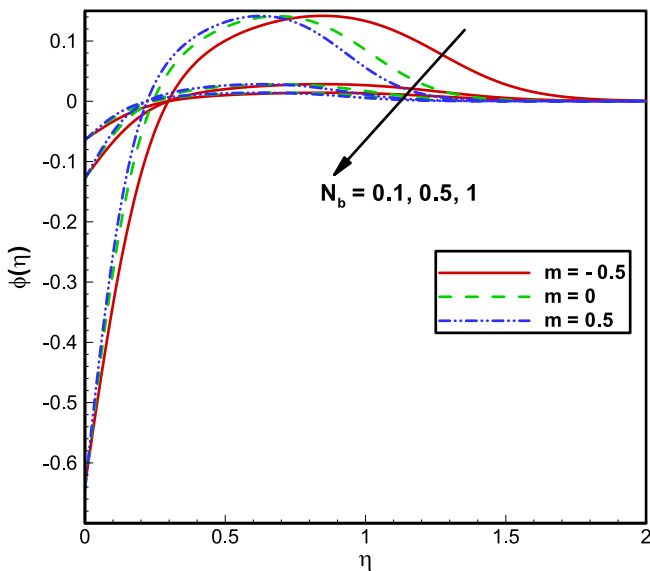**Fig. 3.** Impact of the generalized Prandtl number Pr on the temperature and concentration profiles.

Fig. 4. Impact of the Brownian motion parameter N_b on concentration profile.

render the dependence of the Prandtl number on the nanoparticle concentration. It is revealed that the concentration boundary layer overshoots near the wall for upgraded values of Pr and gradually it lessens away from the boundary.

The consequence of the Brownian motion parameter N_b on the nanoparticle concentration profile is depicted in Fig. 4 for shear thinning, second grade and shear thickening fluids. It is revealed that the uprising values of N_b decreases the nanoparticle concentration and thus a reduction in concentration boundary layer could be seen. The growing values of the Brownian motion parameter interrupt the Brownian motion and thus prevent the diffusion of the nanoparticles in the flow regime which results in the reduction of the concentration of the nanoparticle volume fraction. The variation in temperature profile is negligible corresponding to different values of N_b in correspondence to applicability of the boundary condition proposed by Kuznetsov and Nield [29].

Fig. 5(a) and (b) demonstrates the variation of the temperature and nanoparticle concentration profiles for growing values of the Lewis number Le for shear thinning, second grade and shear thickening fluids. Fig. 5(a) displays that the temperature as well as the thermal boundary layer increases corresponding to escalating values of the Lewis number. However, the behavior is much promi-
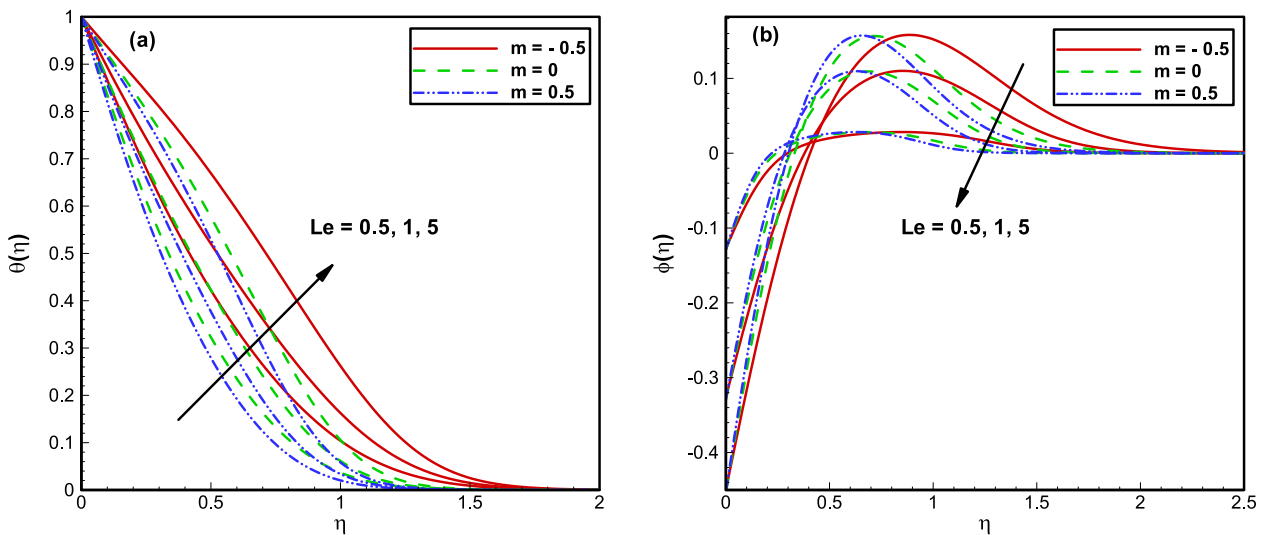

Fig. 5. Impact of the Lewis number Le on the temperature and concentration profiles.
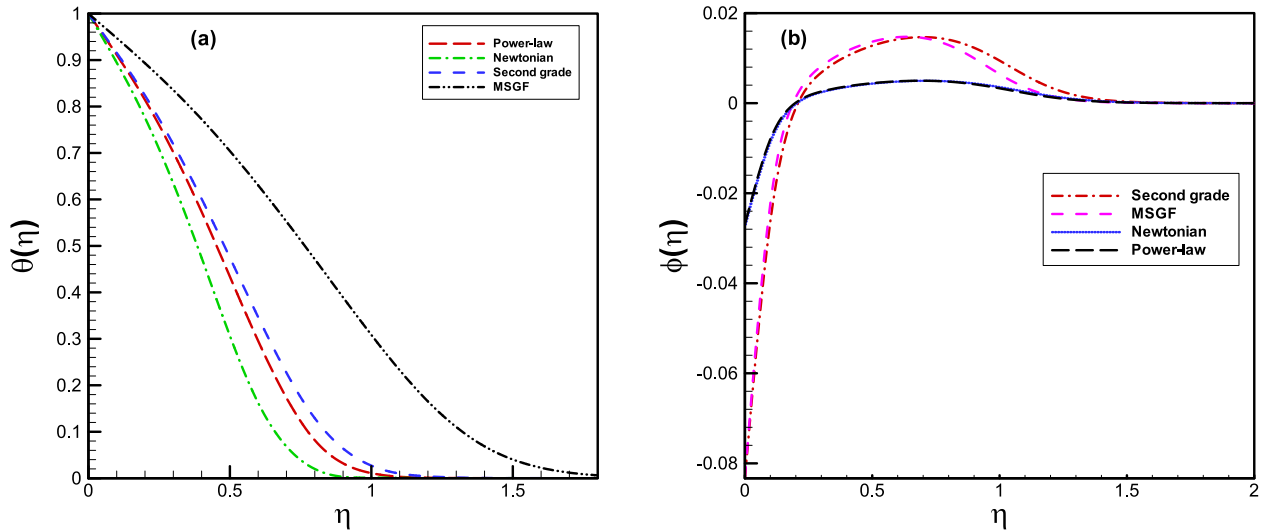
Fig. 6. A comparison of the temperature and concentration profiles of the Newtonian, power-law, second grade and modified second grade nanofluids.
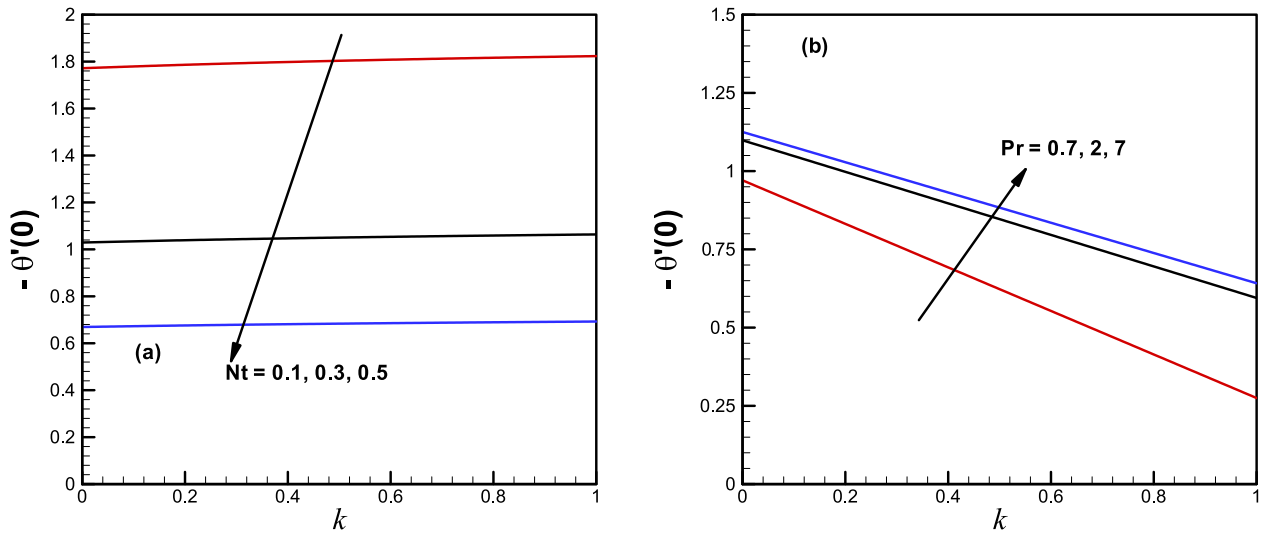

Fig. 7. Impact of the thermophoresis parameter N_t and the generalized Prandtl number Pr on the local Nusselt number when $m = 0.1$ is fixed.

nent for shear-thinning fluid. Fig. 5(b) portrays that the nanoparticle concentration becomes weaker for developing values of the Lewis number. An increase in the Lewis number scales down the molecular diffusivity which compels to decay the concentration boundary layer.

Fig. 6(a) and (b) display the temperature and nanoparticle concentration profiles for the case of the Newtonian nanofluid ($k = 0, m = 0$), the second grade nanofluid ($k \neq 0, m = 0$) and the power-law nanofluid ($m \neq 0, k = 0$) with those of the modified second grade nanofluid, respectively. It is noticeable that the modified second grade nanofluid has the most elevated thermal boundary layer as compared to the other three fluid models. Moreover, it is revealed that the boundary layer thickness increases for the modified second grade nanofluid in comparison with the Newtonian and power-law nanofluids away from the wall. However, the second grade fluid has slightly elevated concentration boundary layer as comparative to the second grade nanofluid.

The significance of the thermophoresis parameter N_t and the generalized Prandtl number Pr on the local Nusselt number is acknowledged in Fig. 7(a) and (b), respectively. It is noticed that

the local Nusselt number is an increasing function of Pr while a decreasing function of N_t. This is due to the fact that for higher values of Pr, the convection process is dominant as compared to conduction which causes an increment in the heat transfer rate. This decline due to the rise in the thermophoresis parameter is a consequence of the stronger thermophoretic force that drives the nanoparticles with high thermal conductivity towards the quiescent fluid from the hot sheet.

Table 2 is constructed to scrutinize the heat transfer rate of the modified second grade nanofluid at the wall Nu_x for various values of Pr, s, N_t, N_b and Le for shear-thinning, second grade and shear-thickening regime. The generalized Prandtl number and the Lewis number have opposite impact on the local Nusselt number. However, the heat transfer rate is invariant for the change in the Brownian motion parameter. Furthermore, the stretching parameter has a descending effect on the local Nusselt number for shear-thinning fluid while opposite trend is observed for the second grade and shear-thickening case. Moreover, the effects are more dominant for shear-thickening fluid as compared to second grade and shear-thinning fluids.

Table 2
Numerical values of the heat transfer rate for various values of Pr, s, N_t, N_b and Le for shear-thinning, second grade and shear-thickening fluids.

Pr	s	N_t	N_b	Le	$-\theta'(0)$		
					$m = -0.5$	$m = 0$	$m = 0.5$
0.7	1	0.5	1	10	0.359850	0.440518	0.471571
2					0.566861	0.704015	0.766499
7					0.602552	0.747405	0.818602
	1				0.538927	0.667694	0.731716
	2.5				0.533084	0.892486	1.051525
	5				0.529190	1.174546	1.440956
		0.1			1.422527	1.761280	1.930712
		0.3			0.827376	1.025791	1.124418
		0.5			0.538233	0.667560	0.731714
			0.5		0.538233	0.667560	0.731714
			1		0.538233	0.667560	0.731714
			2.5		0.538233	0.667560	0.731714
				1	1.053695	1.309358	1.434378
				5	0.626548	0.777770	0.852401
				10	0.538233	0.667560	0.731714

Final remarks

The flow and heat transfer of a modified second grade nanofluid over a non-linearly stretching sheet is investigated for the first time. The analysis is computed by examining the passive control of nanoparticles at the boundary. Numerical solutions of the governing problem are calculated and dependence of the pertinent parameters on the temperature and nanoparticle concentrations are graphically exhibited. The main findings can be listed as:

- The concentration of the nanoparticles decreased with an increase in the Brownian motion parameter while its impact on the temperature and local Nusselt number was negligible.
- The generalized Prandtl number and Lewis number turned to reduction of the thermal and concentration boundary layer. However, their elevated values displayed opposite trend in the case of heat transfer rate.
- Increment in the thermophoretic forces expedited the temperature and nanoparticle concentration. Moreover, an increase in thermophoresis parameter resulted in a decrease of heat transfer rate.
- The escalation in the power-law index and the stretching parameter diminished the thermal and concentration boundary layers. Furthermore, stretching parameter enlarged the temperature and nanoparticle concentration for the case of shear-thinning fluid.

Acknowledgement

References

[1] Choi SUS. Enhancing thermal conductivity of fluids with nanoparticles. ASME's Int Mech Eng 1995;66:99–105.
[2] Buongiorno J. Convective transport in nanofluids. J Heat Transfer 2006;128:240–50.
[3] Kim SJ, Bang IC, Buongiorno J, Hu LW. Surface wettability change during pool boiling of nanofluids and its effect on critical heat flux. Int J Heat Mass Transfer 2007;50:4105–16.
[4] Kuznetsov AV, Nield DA. Natural convective boundary-layer flow of a nanofluid past a vertical plate. Int J Therm Sci 2010;49:243–7.
[5] Khan WA, Pop I. Boundary-layer flow of a nanofluid past a stretching sheet. Int J Heat Mass Transfer 2010;53:2477–83.
[6] Gorder RAV, Sweet E, Vajravelu K. Nano boundary layers over stretching surfaces. Commun Nonlinear Sci Numer Simul 2010;15:1494–500.
[7] Roberts NA, Walker DG. Convective performance of nanofluids in commercial electronics cooling systems. Appl Therm Eng 2010;30:2499–504.
[8] Makinde OD, Aziz A. Boundary layer flow of a nanofluid past a stretching sheet with a convective boundary condition. Int J Therm Sci 2011;50:1326–32.
[9] Aziz A, Khan WA. Natural convective boundary layer flow of a nanofluid past a convectively heated vertical plate. Int J Therm Sci 2012;52:83–90.
[10] Das K, Duari PR, Kundu PK. Nanofluid flow over an unsteady stretching surface in presence of thermal radiation. Alex Eng J 2014;53:737–45.
[11] Aly EH, Vajravelu K. Exact and numerical solutions of MHD nano boundary-layer flows over stretching surfaces in a porous medium. Appl Math Comput 2014;232:191–204.
[12] Mabood F, Mastroberardino A. Melting heat transfer on MHD convective flow of a nanofluid over a stretching sheet with viscous dissipation and second order slip. J Taiwan Inst Chem Eng 2015;57:62–8.
[13] Haq RU, Nadeem S, Khan ZH, Akbar NS. Thermal radiation and slip effects on MHD stagnation point flow of nanofluid over a stretching sheet. Physica E 2015;65:17–23.
[14] Khan M, Manzur M, $$$Rahman Mu. Boundary layer flow and heat transfer of cross fluid over a stretching sheet, Thermal Science, https://doi.org/10.2298/TSCI160919111K
[15] Khan M, Manzur M, Rahman Mu. On axisymmetric flow and heat transfer of cross fluid over a radially stretching sheet. Results Phys 2017;7:3767–72.
[16] Manzur M, Khan M, Rahman MU. Mixed convection heat transfer to cross fluid with thermal radiation: effects of buoyancy assisting and opposing flows. Int J Mech Sci 2018. https://doi.org/10.1016/j.ijmecsci.2018.02.010.
[17] Shahzad A, Ali R, Khan M. On the exact solution for axisymmetric flow and heat transfer over a nonlinear radially stretching sheet. Chin Phys Lett 2012;29. 084705-4.
[18] Shahzad A, Ali R. Approximate analytic solution for magneto-hydrodynamic flow of a non-Newtonian fluid over a vertical stretching sheet. Can J Pure Appl Sci 2012;2:202–15.
[19] Sokolov A, Ali R, Turek S. An AFC-stabilized implicit finite element method for partial differential equations on evolving-in-time surfaces. J Comput Appl Math 2014;289:101–15.
[20] Ahmed J, Shahzad A, Khan M, Ali R. A note on convective heat transfer of an MHD Jeffrey fluid over a stretching sheet. AIP Adv 2015;5:117117.
[21] Ali R, Shahzad A, Khan M, Ayub M. Analytic and numerical solutions for axisymmetric flow with partial slip. Eng Comput 2016;32:149–54.
[22] Ahmed J, Begum A, Shahzad A, Ali R. MHD axisymmetric flow of power-law fluid over an unsteady stretching sheet with convective boundary conditions. Results Phys 2016;6:973–81.
[23] Hayat T, Ali S, Farooq MA, Alsaedi A. On comparison of series and numerical solutions for flow of Eyring-Powell fluid with Newtonian heating and internal heat generation/absorption. PLoS One 2015;10:e0129613.
[24] Alsaedi A, Alsaadi FE, Ali S, Hayat T. Stagnation point flow of Burgers' fluid and mass transfer with chemical reaction and porosity. J Mech 2013;29:453–60.
[25] Hayat T, Ali S, Awais M, Alsaedi A. Joule heating effects in MHD flow of burgers' fluid. Heat Transfer Res 2016;47:1083–92.
[26] Man CS, Sun QX. On the significance of normal stress effects in the flow of glaciers. J Glaciol 1987;33:268–73.
[27] Aksoy Y, Pakdemirli M, Khalique CM. Boundary layer equations and stretching sheet solutions for the modified second grade fluid. Int J Eng Sci 2007;45:829–41.
[28] Khan M, Rahman M. Flow and heat transfer to modified second grade fluid over a non-linear stretching sheet. AIP Adv 2015;5:087157.
[29] Rahman MU, Manzur M, Khan M. Mixed convection heat transfer to modified second grade fluid in the presence of thermal radiation. J Mol Liq 2016;223:217–23.
[30] Rahman MU, Manzur M, Khan M. Homogeneous-heterogeneous reactions in modified second grade fluid over a non-linear stretching sheet with Newtonian heating. Results Phys 2017;7:4364–70.
[31] Khan M, Rahman MU, Manzur M. Axisymmetric flow and heat transfer to modified second grade fluid over a radially stretching sheet. Results Phys 2017;7:878–89.
[32] Kuznetsov AV, Nield DA. Natural convective boundary-layer flow of a nanofluid past a vertical plate: a revised model. Int J Therm Sci 2014;77:126–9.
[33] Mustafa M, Khan JA, Hayat T, Alsaedi A. Analytical and numerical solutions for axisymmetric flow of nanofluid due to non-linearly stretching sheet. Int J Non Linear Mech 2015;71:22–9.